# Electronic Supplementary Information

## Templating the 3D structure of conducting polymers with self-assembling peptides

*Taylor J. Blatz,*[a] *Melany M. Fry,*[a] *Ellie I. James,*[a] *Tyler J. Albin,*[a] *Zoe Pollard,*[b] *Tim Kowalczyk* [a,b] *and Amanda R. Murphy*[a,*]

[a]Department of Chemistry and [b]Advanced Materials Science and Engineering Center, Western Washington University, 516 High St., Bellingham, WA 98225, United States

*E-mail: amanda.murphy@wwu.edu

### Supplementary Tables and Figures

**Table S1.** Calculated binding energies (in kcal/mol) of DFTB3-optimized parallel and anti-parallel dimer conformations of hexyl-GAGA and hexyl-GAGA-EDOT.

| hexyl-GAGA | parallel | anti-parallel |
|---|---|---|
| DFTB3 | -30.4 | -26.0 |
| B3LYP-D | -29.9 | -26.4 |
| ωB97X-D | -26.2 | -23.1 |

| hexyl-GAGA-EDOT | parallel | anti-parallel |
|---|---|---|
| DFTB3 | -43.1 | -32.4 |
| B3LYP-D | -39.4 | -29.7 |
| ωB97X-D | -38.5 | -27.4 |

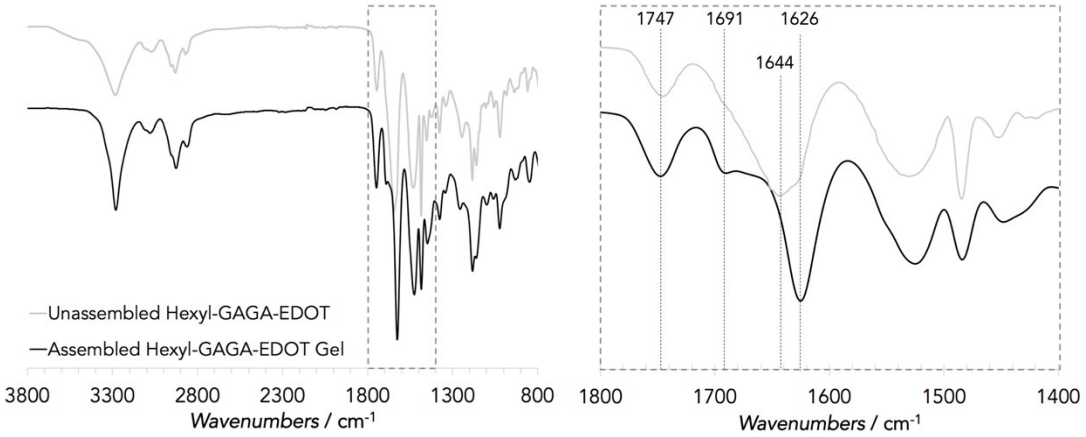


**Fig. S1** ATR-FTIR spectra of hexyl-GAGA-EDOT before (lyophilized powder) and after assembly (gelled in ethyl acetate then dried). Full spectra are given on the left, and an expansion of the carbonyl region is on the right. The amide C=O stretch at 1640-1650 $cm^{-1}$ is indicative of a random coil type structure, while a C=O stretch at 1626 $cm^{-1}$ with a shoulder at 1691 $cm^{-1}$ are indicative of an anti-parallel beta sheet structure. The ester C=O from the peptide linkage to EDOT was also prominent at 1747 $cm^{-1}$.

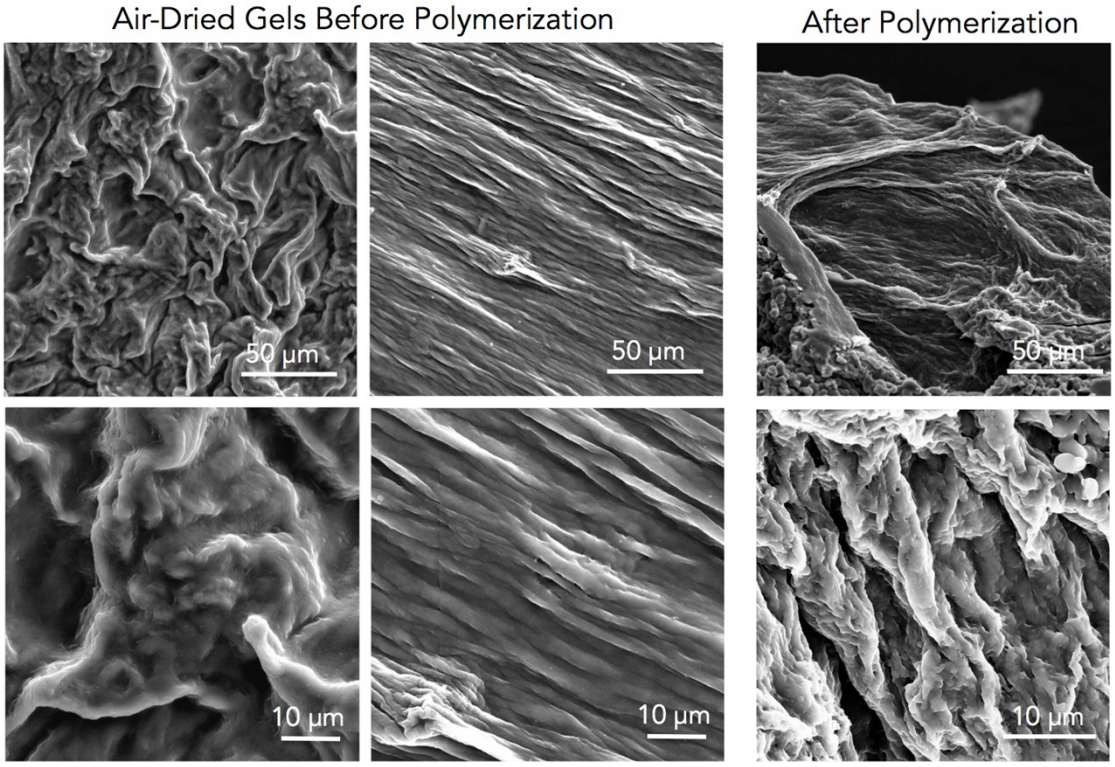


**Fig. S2** SEM images of air-dried gels of hexyl-GAGA-EDOT:EDOT-OH before and after polymerization. Wrinkled and aligned regions were present in the samples. While the structure heavily compacted during drying, some fibers can be seen embedded in the surface.

As noted in the text, while the gels formed best in ethyl acetate, gels often collapsed during polymerization in this solvent. As shown in Figure S3a, when the $FeCl_3$ oxidant was added (yellow color), gels would collapse after ~ 1 d, forming a blue-green powder on the bottom of the vial. After isolating and washing this powder, ATR-FTIR analysis indicated that the peptide was still present, as C=O peaks for the ester and amide groups were clearly visible (Fig. S3b). However, the C=O peak had shifted back to 1643 $cm^{-1}$, the value observed in the lyophilized peptide before assembly (Fig. S1), indicating that the beta sheet assembly was completely disrupted. SEM imaging revealed that the powder was comprised of aggregated spherical particles that were remarkably consistent in diameter (~3-4 µm). While these spheres were intriguing, they were not pursued further for the purposes of this manuscript. However, these results demonstrate the necessity to maintain the 3D peptide structure throughout the polymerization if a fibrous structure is desired.

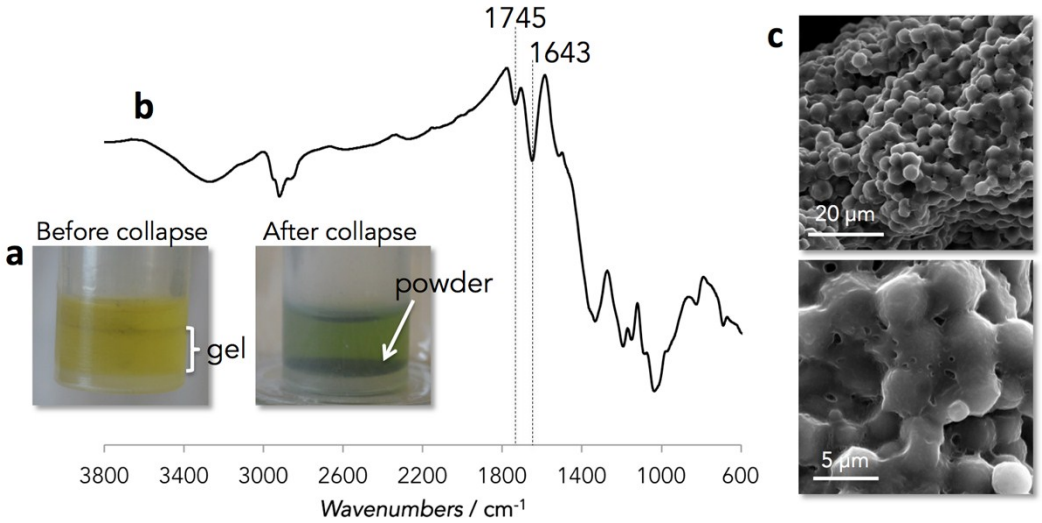


**Fig. S3** (a) Photographs of a gel before and after it collapsed during polymerization. (b) ATR-FTIR spectrum of the powder collected from a collapsed gel. The shift in the C=O bond to higher wavenumbers indicated that the peptide was no longer assembled. (c) SEM images of the powder collected from a collapsed gel. Aggregated spherical particles ~3-4 µm in diameter were observed.

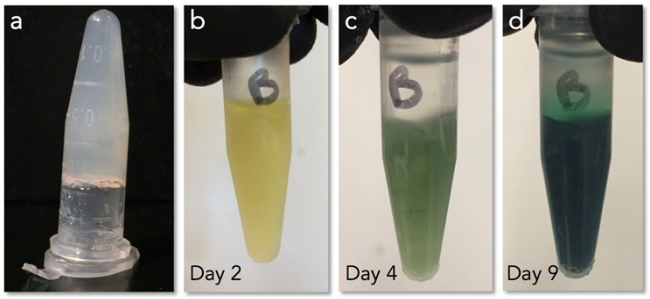


**Fig. S4** Photographs of a gel (a) before $FeCl_3$ was added, (b) after the $FeCl_3$ solution (yellow) had been injected and allowed to permeate throughout the gel for 24 h at -20 °C, (c) after polymerization at RT for 2 days and (d) 7 days. As the polymerization progresses, the gels turn from yellow to green to bluish-black.

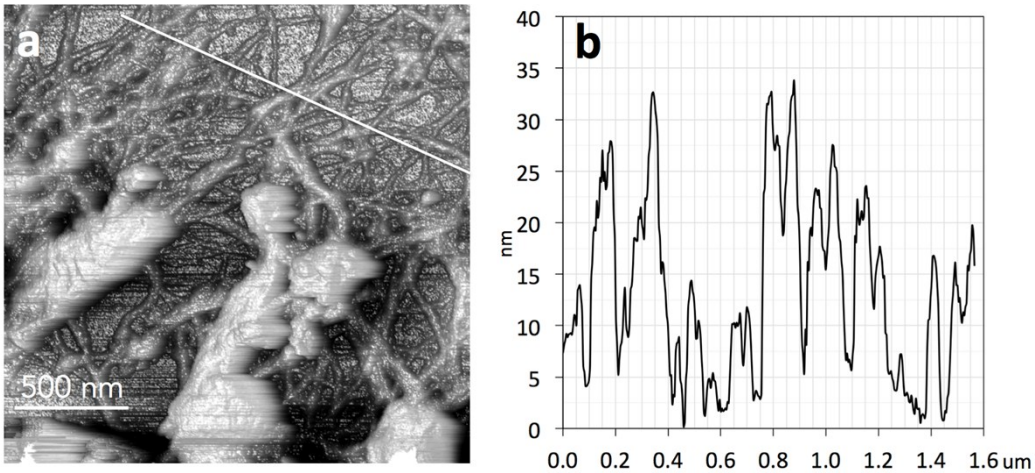


**Fig. S5** (a) AFM image of another polymerized gel that was suspended and diluted in ether prior to casting on mica. Fibers, fiber bundles and aggregates were observed. (b) Height profile of the fibers along the white line shown in image (a).

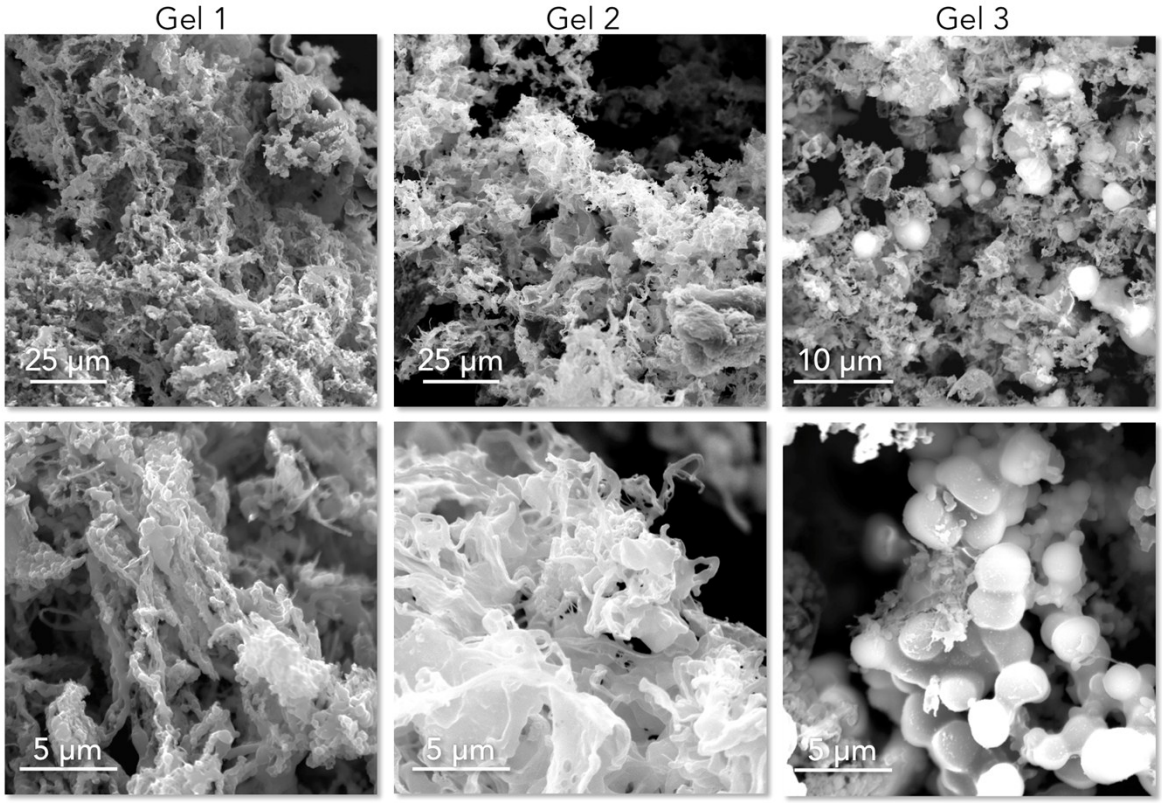


**Fig. S6** SEM images of several polymerized gel samples prepared in the same manner to show the range of morphologies observed. Samples mostly consisted of fibers, bundles and sheets, but a few samples contained some embedded particles similar to particles observed when gels collapsed during polymerization (Fig. S3).

**Table S2.** Conductivity measurements of gels spread and dried on interdigitated gold electrodes (Mylar substrate, 40 electrode pairs with 20 µm width and spacing).

| Film # | Average resistance (Ohms) | Cell constant ($cm^{-1}$) | Resistivity (Ohm-cm) | Conductivity (S/cm) |
|---|---|---|---|---|
| **1** | 68 | 0.0789 | 865 | 1.1E-3 |
| **2** | 270 | 0.0789 | 3428 | 2.9E-4 |
| **3** | 417 | 0.0789 | 5296 | 1.9E-4 |
| **4** | 1421 | 0.0789 | 18027 | 5.5E-5 |
| **5** | 644 | 0.0789 | 8161 | 1.2E-4 |
| **AVERAGE** | 564 | - | 7155 | 3.5E-4 |

**Table S3.** Conductivity measurements of gels spread on glass slides and evaluated with a 4-point probe.

| Film # | Sheet resistivity (Ohms-sq) | Average film thickness* (cm) | Resistivity (Ohm-cm) | Conductivity (S/cm) |
|---|---|---|---|---|
| **1** | 148,000 | 0.0154 | 2279 | 4.4E-4 |
| **2** | 339,000 | 0.0154 | 5221 | 1.9E-4 |
| **AVERAGE** | 243,500 | - | 3750 | 3.2E-4 |

*The three-dimensional, bumpy nature of the films led to large variations in film thickness. The majority of the films were 154 ± 65 µm, but large clumps up to 600 µm were occasionally observed. Therefore, the conductivity values measured with this method range from 8E-4 to 8E-5 S/cm if using the thinnest and thickest film sections, respectively. These values were, however, consistent with the values measured with the interdigitated electrodes.

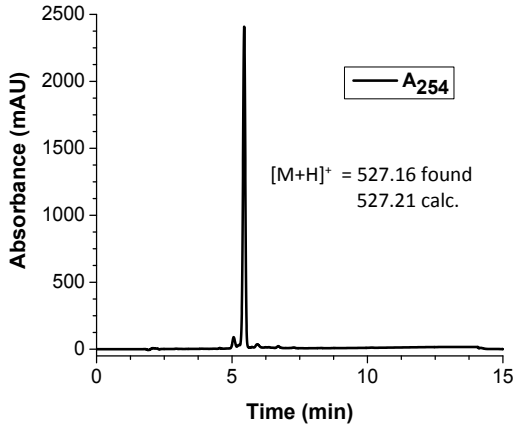


**Fig. S7.** RP-HPLC chromatogram of the hexyl-GAGA-EDOT product along with the associated LC-ESI-MS data.

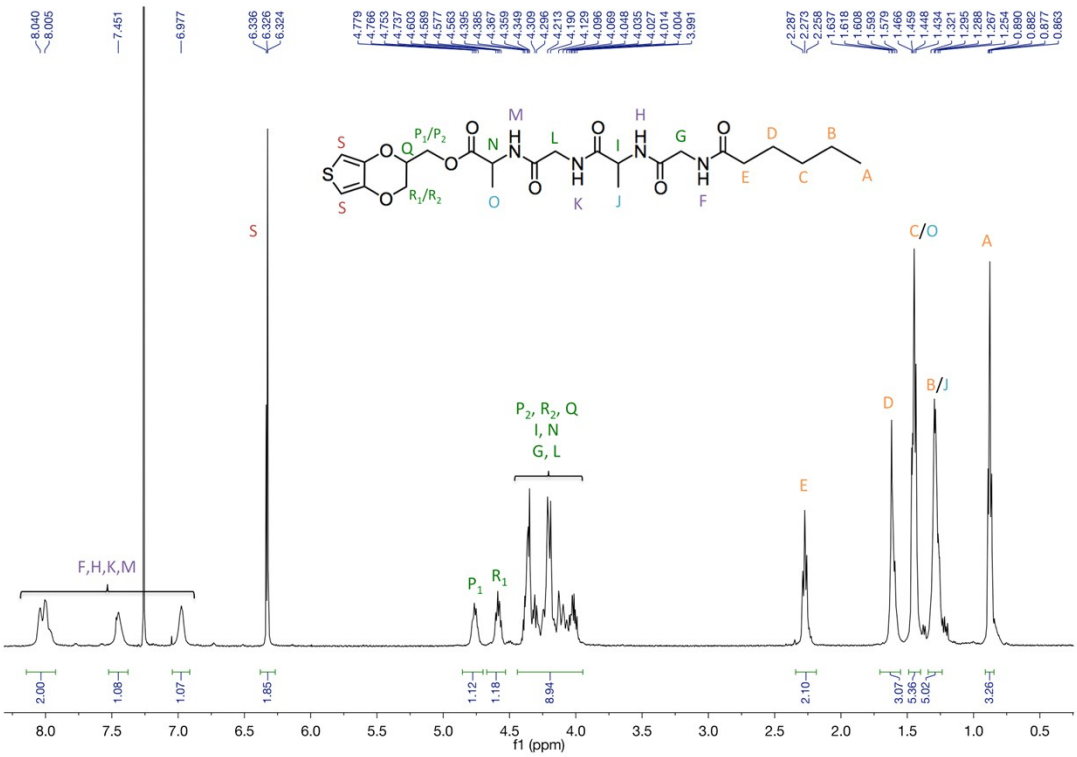


**Fig. S8.** $^{1}$H NMR spectrum of hexyl-GAGA-EDOT in $CDCl_3$.

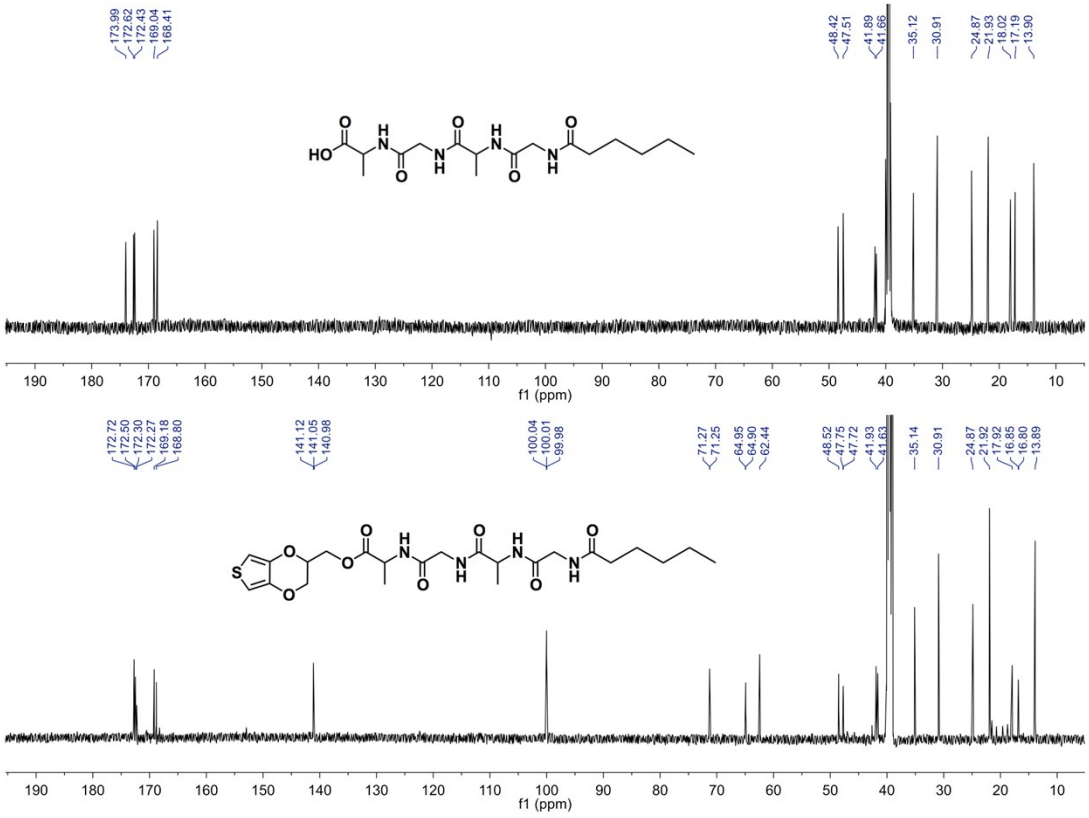


**Fig. S9.** $^{13}$C NMR spectra of hexyl-GAGA and hexyl-GAGA-EDOT in DMSO-$d_6$.

**Additional Molecular Dynamics Simulation Details**

The three peptide-CP structures described in Fig. 5 of the manuscript were solvated separately in periodic boxes of water and of diethyl ether. The peptide-CP solute and diethyl ether solvent were modeled using the OPLS/AA force field,[1] while the SPC model was adopted for water.[2] After energy minimization and *NPT* equilibration dynamics at STP, production simulations for each structure/solvent pair were performed over 1 ns using the velocity Verlet integrator[3] and an integration time step of 1 fs. Electrostatic interactions were treated via the particle mesh Ewald algorithm[4] while velocity-rescaling temperature coupling[5] was adopted to ensure sampling of the canonical ensemble at $T$ = 298 K. Hydrogen bonding in the sampled configurations was quantified using standard geometrical criteria adopted in the GROMACS `hbond` program.[6] The snapshots in Fig. 5 were rendered using the VMD package.[7]

**Additional References for ESI**


1. G. A. Kaminski, R. A. Friesner, J. Tirado-Rives, and W. L. Jorgensen, *J. Phys. Chem. B*, 2001, **105**, 6474-6487.

2. H. J. C. Berendsen, J. R. Grigera, and T. P. Straatsma, *J. Phys. Chem.* 1987, **91**, 6269-6271.

3. W. C. Swope, H. C. Andersen, P. H. Berens, K. R. Wilson, *J. Chem. Phys.* 1982, **76**, 637-649.

4. T. Darden, D. York, L. Pedersen, *J. Chem. Phys.* 1993, **98**, 10089-10092.

5. G. Bussi, D. Donadio, M. Parrinello, *J. Chem. Phys.* 2007, **126**, 014101.

6. M.J. Abraham, D. van der Spoel, E. Lindahl, B. Hess, and the GROMACS development team, GROMACS User Manual v. 2016.3.

7. W. Humphrey, A. Dalke, K. Schulten, *J. Mol. Graph.* 1996, **14**, 33-38.